UNCLASSIFIED
SECURITY CLASSIFICATION OF THIS PAGE

REPORT DOCUMENTATION PAGE

Form Approved OMB No. 0704-0188

DTIC ELECTE OCT 4 1989 D

AD-A213 113

1a. REPORT SECURITY CLASSIFICATION: Unclassified	1b. RESTRICTIVE MARKINGS
2a.	3. DISTRIBUTION/AVAILABILITY OF REPORT: Approved for public release; distribution is unlimited.
4. PERFORMING ORGANIZATION REPORT NUMBER(S)	5. MONITORING ORGANIZATION REPORT NUMBER(S): AFATL-TP-89-16
6a. NAME OF PERFORMING ORGANIZATION: Aerodynamics Branch, Aeromechanics Division — 6b. OFFICE SYMBOL (If applicable): AFATL/FXA	7a. NAME OF MONITORING ORGANIZATION: Aerodynamics Branch, Aeromechanics Division
6c. ADDRESS (City, State, and ZIP Code): Air Force Armament Laboratory, Eglin AFB FL 32542-5434	7b. ADDRESS (City, State, and ZIP Code): Air Force Armament Laboratory, Eglin AFB FL 32542-5434
8a. NAME OF FUNDING/SPONSORING ORGANIZATION: Aeromechanics Division — 8b. OFFICE SYMBOL (If applicable): AFATL/FXA	9. PROCUREMENT INSTRUMENT IDENTIFICATION NUMBER
8c. ADDRESS (City, State, and ZIP Code): Air Force Armament Laboratory, Eglin AFB FL 32542-5434	10. SOURCE OF FUNDING NUMBERS

PROGRAM ELEMENT NO.	PROJECT NO.	TASK NO	WORK UNIT ACCESSION NO.
62602F	2567	03	22

11. TITLE (Include Security Classification)
Aerodynamics of Missiles with Offset Fin Configurations

12. PERSONAL AUTHOR(S)
Gregg L. Abate, and Wayne H. Hathaway

13a. TYPE OF REPORT	13b. TIME COVERED	14. DATE OF REPORT (Year, Month, Day)	15. PAGE COUNT
Paper	FROM Oct 87 TO Aug 89	September 1989	9

16. SUPPLEMENTARY NOTATION
AIAA Atmospheric Flight Mechanics Symposium
Boston, Massachusetts - August 1989

17. COSATI CODES		
FIELD	GROUP	SUB-GROUP

18. SUBJECT TERMS (Continue on reverse if necessary and identify by block number)
Offset Fins, Aerodynamics, Missile Stability, Dynamic Stability, Flexible Fins, Side Moments

19. ABSTRACT (Continue on reverse if necessary and identify by block number)
Subsonic and transonic aerodynamic data for offset fin configurations are presented. Free-flight aeroballistic tests to obtain this data were conducted at atmospheric pressure over a Mach number range of 0.6 to 1.6. The aerodynamic coefficients and derivatives presented were extracted from the position-attitude-time histories of the experimentally measured trajectories using nonlinear numerical integration data reduction routines. Results of this testing and analysis show the static and dynamic stability variations for four different fin offset configurations. The presence of a side moment dependent on pitch angle results in dynamic instability under certain conditions. The stability boundaries associated with this side moment are mapped. Designers should consider this moment whenever offset fins are utilized.

20. DISTRIBUTION/AVAILABILITY OF ABSTRACT: ☐ UNCLASSIFIED/UNLIMITED ☒ SAME AS RPT. ☐ DTIC USERS	21. ABSTRACT SECURITY CLASSIFICATION: Unclassified
22a. NAME OF RESPONSIBLE INDIVIDUAL: Gregg L. Abate	22b. TELEPHONE (Include Area Code): (904) 882-4085 — 22c. OFFICE SYMBOL: AFATL/FXA

DD Form 1473, JUN 86 — Previous editions are obsolete.

SECURITY CLASSIFICATION OF THIS PAGE
UNCLASSIFIED

89 10 4 029

AERODYNAMICS OF MISSILES WITH OFFSET FIN CONFIGURATIONS

Gregg L. Abate*
Aerodynamics Branch
Aeromechanics Division
Air Force Armament laboratory
Eglin AFB, FL

and

Wayne H. Hathaway**
Arrow Tech Associates
Lakewood Commons
South Burlington, VT

Abstract

Subsonic and transonic aerodynamic data for offset fin configurations are presented. Free-flight aeroballistic tests to obtain this data were conducted at atmospheric pressure over a Mach number range of 0.6 to 1.6. The aerodynamic coefficients and derivatives presented were extracted from the position-attitude-time histories of the experimentally measured trajectories using nonlinear numerical integration data reduction routines. Results of this testing and analysis show the static and dynamic stability variations for four different fin offset configurations. The presence of an side moment dependent on pitch angle results in dynamic instability under certain conditions. The stability boundaries associated with this side moment are mapped. Designers should consider this *moment whenever offset fins are utilized.*

Nomenclature

A	= reference area
ABARM	= max total angle of attack
a_c	= Coriolis acceleration
C_l	= roll moment coefficient
C_{lp}	= spin decay roll moment coefficient
C_l	= induced roll moment coefficient derivative
$C_{m\alpha}$	= pitching moment coefficient derivative per sin α
$C_{m\dot{\alpha}}$	= pitching moment coefficient derivative per sin $\dot{\alpha}$
C_{mq}	= pitch damping derivative
$C_{m\delta}$	= moment due to trim
$C_{m\alpha 3}, C_{m\alpha 5}$	= cubic and fifth order coefficient derivatives
$C_{m\,M}$	= slope of pitching moment versus Mach number
C_N	= normal force coefficient
$C_{N\alpha}$	= normal force coefficient derivative per sin
$C_{N\delta}$	= normal force due to trim
$C_{N\alpha 3}, C_{N\alpha 5}$	= cubic and fifth order normal force coefficients
C_n, Cnsm	= side moment coefficient
$C_{n\alpha}$	= slope of side moment versus sin
$C_{np\alpha}$	= Magnus moment derivative
$C_{n\gamma\alpha}$	= induced side moment derivative
C_{xo}	= axial force coefficient at zero angle angle of attack
$C_{x\alpha 3}$	= squared axial force coefficient versus $\sin^3$
C_{xM}	= slope of axial force versus Mach number
C_{Yp}	= Magnus force coefficient
C_Y	= side force coefficient
d	= body diameter
DBSQ	= effective mean angle of attack squared
g	= acceleration due to gravity
I_x, I_y	= moments of inertia about the x and y axis
l, m, n	= aerodynamic roll, pitch, and yaw moments
$\overline{m}$	= model mass
M	= Mach number
p, q, r	= roll, pitch, and yaw angular velocity components
$\overline{q}$	= dynamic pressure
ρ	= air density
u, v, w	= missile velocity components in fixed plane coordinates
V	= total velocity
α	= total angle of attack
γ	= *aerodynamic roll angle*
θ, ψ, ϕ	= missile orientation angles
λ_1, λ_2	= linear theory vector damping rates

Superscript

$-$	= total coefficient
$\cdot$	= first derivative WRT time

* Aerospace Engineer, Member AIAA

** Advanced Munitions Engineer, Member AIAA

Introduction

In an effort to develop innovative missile designs, the concept of 'offset fins' has been proposed. Unlike traditional missiles with fins perpendicular to the body, offset fin configurations have fins at angles less than 90 degrees from a plane tangent to the cylindrical body at the fin interface. For tube launched applications, this provides significant advantages in packaging and design simplicity.

To better understand the aerodynamics and stability characteristics of this class of configurations, the Aerodynamics Branch of the Air Force Armament Laboratory conducted a series of free flight tests to experimentally investigate the aerodynamics.

The purpose of the research testing reported herein was to investigate four offset fin configurations of 60 deg, 45 deg, 30 deg, and 0 deg at Mach numbers ranging from 0.6 to 1.6. The test program was conducted in the Aeroballistic Research Facility (ARF), Eglin Air Force Base, Florida.

Facilities & Test Models

Free Flight Range

The Aeroballistic Research Facility[1] (ARF) is an enclosed concrete structure used to examine the exterior ballistics of various free-flight munitions. The facility contains a gun room, control room, model measurement room, blast chamber, and an instrumented range. The range atmosphere is controlled and closely monitored.

The 207 meter range has a 3.66 meter cross-section for the first 69 meters and a 4.88 meter square cross-section for the remaining length. The range has 131 locations available as instrumentation sites and each location has a physical separation of 1.52 meters. Presently 50 of these sites are used to house fully instrumented orthogonal shadowgraph stations. At each of these stations, the maximum shadowgraph window (an imaginary circle in which a projectile will cast a shadow on two orthogonal reflective screens) is 2.13 meters in diameter. The orthogonal photographs of the model's shadow can be used to determine the spatial position and angular orientation of the model at each of the 50 instrumented sites. The discrete time dynamic data of positions and orientations are then used by the data reduction program to determine the aerodynamic forces and moments acting on the model for that flight.

Models & Test Conditions

The research configuration which is referred to as an offset fin configuration is illustrated in Figure 1. This test model is a 10-caliber ogive-cylinder-tail configuration. It has a 2.5 caliber tangent ogive, and the afterbody is a right circular cylinder 7.5 calibers in length. The fins are of a double wedge clipped delta configuration whose trailing edges fit flush with the base of the model.

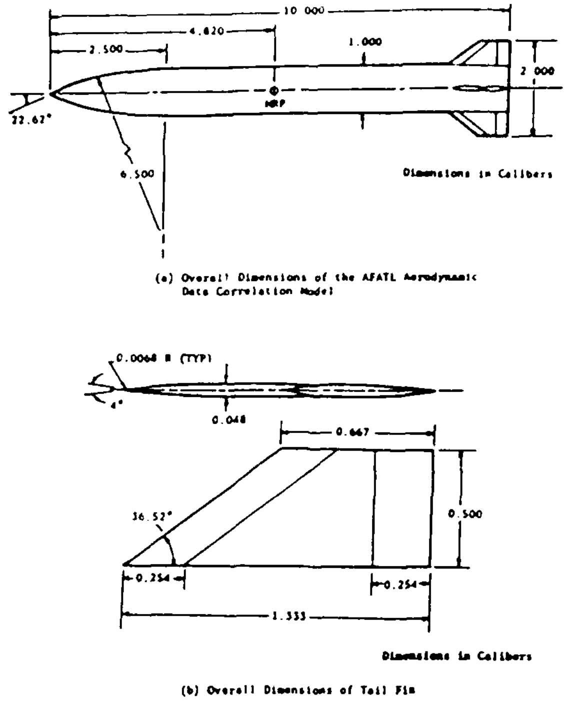

Figure 1. Air Force Basic Research Configuration (Ref. 4)

This model, with fins in the conventional 90 deg orientation, has been the subject of considerable experimental research in both wind tunnel and ballistic spark range testing. Therefore, a large pre-existing data base is available for the 90 deg offset. Reference 2 is an excellent source for both wind tunnel and range data.

Figure 2 illustrates the fin offsets which are the subject of this investigation. Table 1 summarizes the typical mass properties of the test models.

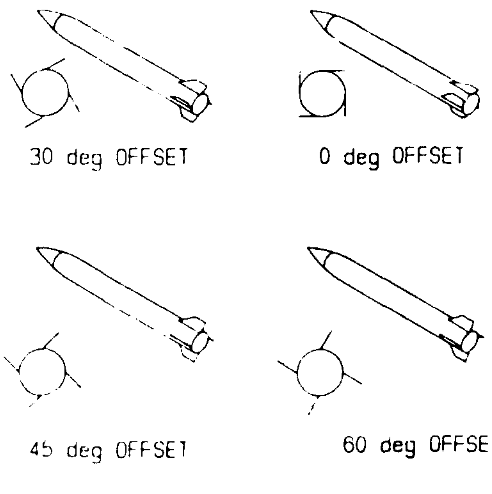

Figure 2. Offset Fin Configurations Tested

Table 1. Physical Properties

	0-degree	30,45,60-degree
Diameter, cm.	1.91	1.91
Mass, gm.	189.0	127.1
I_x, gm-cm^2	89.2	63.8
I_y, gm-cm^2	3889	3889
Length, cm.	19.1	19.1
C.G., percent from nose	39.7	49.1

Roll pins were installed in each test model to acquire roll orientation data. This data is critical towards determining any aerodynamic trends as a function of roll angle (i.e. trims and induced forces and moments).

Data Analysis

Extraction of the aerodynamic coefficients and derivatives is the primary goal in analyzing the trajectories measured in the ARF. This is accomplished by using ARFDAS described in References 3 and 4. ARFDAS incorporates a standard linear theory analysis (References 5 and 6) and a six-degree-of-freedom (6DOF) numerical integration technique. The 6DOF routine incorporates the Maximum Likelihood Method (MLM) to match the theoretical trajectory to the experimentally measured trajectory. The MLM is an iterative procedure that adjusts the aerodynamic coefficients to maximize a likelihood function. The use of this likelihood function eliminates the inherent assumption in least squares theory that the magnitude of the measurement noise must be consistent between dynamic parameters (irrespective of units). In general, the aerodynamics can be nonlinear functions of the angle of attack, Mach number, and aerodynamic roll angle.

ARFDAS represents a complete ballistic range data reduction system capable of analyzing both symmetric and asymmetric bodies. The essential steps of the data reduction system are to: (1) assemble the dynamic range data (time, position, attitude), physical properties, and atmospheric conditions, (2) perform linear theory analysis, (3) perform 6DOF analysis for final aerodynamics. These steps have been integrated into ARFDAS to provide the test engineer with a convenient and efficient means of interaction. At each step in the analysis, permanent records for each flight are maintained such that subsequent analysis with data modifications are much faster.

Each model tested in the ARF was initially analyzed separately, then some were combined in groups for simultaneous analysis using the multiple fit capability. This provides a common set of aerodynamics that match each of the separately measured position-attitude-time profiles. The multiple fit approach provides a more complete spectrum of angle of attack and roll orientation than would be available from any one trajectory considered separately. This increases the probability that the determined coefficients define the model's aerodynamics over the entire range of trajectories.

Equations of Motion

The aerodynamic data presented in this paper were obtained using the fixed plane 6DOF analysis (MLMFXPL). The equations of motion are derived with respect to a fixed plane coordinate system. The x-axis points downrange, the y-axis points to the left looking downrange, and the z-axis points up. The 6DOF differential equations of motion in this system are:

$$\dot{u} = g \sin\theta - qw + rv - a_{cu} + \frac{F_x}{m} \qquad (1)$$

$$\dot{v} = -ru - r \tan\theta - a_{cv} + \frac{F_y}{m} \qquad (2)$$

$$\dot{w} = -g \cos\theta + rv \tan\theta + qu - a_{cw} + \frac{F_z}{m} \qquad (3)$$

$$\dot{p} = \frac{l}{I_x} \qquad (4)$$

$$\dot{q} = -r^2 \tan\theta - \left(\frac{I_x}{I_y}\right) rp + \frac{m}{I_y} \qquad (5)$$

$$\dot{r} = qr \tan\theta + \left(\frac{I_x}{I_y}\right) qp + \frac{n}{I_y} \qquad (6)$$

Once the aerodynamic forces and moments are determined, the solution of Equations 1-6 will define the 6DOF flight motion with respect to the fixed plane coordinate system. Since the position-attitude measurements, as acquired from the ballistic spark range, are relative to the Earth-fixed coordinate system, additional transformation equations are required. Equations 7-12 are these transformation equations shown below in terms of the fixed plane Euler angles (θ, ψ) and the angle of rotation about the missile axis (ϕ).

$$\dot{x} = u \cos\theta \cos\psi - v \sin\psi + w \sin\theta \cos\psi \qquad (7)$$

$$\dot{y} = u \cos\theta \sin\psi + v \cos\psi + w \sin\theta \sin\psi \qquad (8)$$

$$\dot{z} = -u \sin\theta + w \cos\theta \qquad (9)$$

$$\dot{\theta} = q \qquad (10)$$

$$\dot{\psi} = \frac{r}{\cos\theta} \qquad (11)$$

$$\dot{\phi} = p + r \tan\theta \qquad (12)$$

Coriolis accelerations (a_{cu},a_{cv},a_{cw}) are also included in Equations 1-3. Equations 1-12 are numerically integrated using a fourth-order Runge-Kutta scheme.

Aerodynamic Model

Previous testing of wraparound fins have shown instabilities in the form of an out of plane side moment ($C_{n\alpha}$) leading to undamped coning motions which are highly Mach number dependent, Reference 7 contains test results from prior wraparound fin testing.

The aerodynamic coefficients and derivatives, shown in Equations 13-18, were expanded as functions of Mach number, sine of the total angle of attack, and the aerodynamic roll angle. These expansions are shown in detail in Reference 8. However, the side moment expansion was assumed to be linear (i.e. $\bar{C}_{n\alpha} = C_{n\alpha}$).

The aerodynamic forces and moments are defined as follows:

$$F_X = -\bar{q}AC_X \qquad (13)$$

$$F_Y = \bar{q}A\Big[-\bar{C}_{N\alpha}\frac{v}{V} + \frac{pd}{2V}\bar{C}_{Yp\alpha}\frac{w}{V} + \bar{C}_{Y\gamma\alpha}\frac{w}{V} + (\bar{C}_{N\delta}\delta_A)\sin\phi - (\bar{C}_{N\delta}\delta_B)\cos\phi \Big] \qquad (14)$$

$$F_Z = \bar{q}A\Big[-\bar{C}_{N\alpha}\frac{w}{V} - \frac{pd}{2V}\bar{C}_{Yp\alpha}\frac{v}{V} - \bar{C}_{Y\gamma\alpha}\frac{v}{V} - (\bar{C}_{N\delta}\delta_A)\sin\phi - (\bar{C}_{N\delta}\delta_B)\cos\phi \Big] \qquad (15)$$

$$l = \bar{q}A\Big[\frac{pd}{2V}\bar{C}_{lp} + \bar{C}_l \Big] \qquad (16)$$

$$m = \bar{q}Ad\Big[\bar{C}_{m\alpha}\frac{w}{V} + \frac{qd}{2V}\bar{C}_{mq} + \frac{pd}{2V}\bar{C}_{np\alpha}\frac{v}{V} + \bar{C}_{n\gamma\alpha}\frac{v}{V} + \bar{C}_{n\alpha}\frac{v}{V} + \bar{C}_{m\delta}\delta_A\cos\phi - \bar{C}_{m\delta}\delta_B\sin\phi \Big] \qquad (17)$$

$$n = \bar{q}Ad\Big[-\bar{C}_{m\alpha}\frac{v}{V} + \frac{rd}{2V}\bar{C}_{mq} + \frac{pd}{2V}\bar{C}_{np\alpha}\frac{w}{V} + \bar{C}_{n\gamma\alpha}\frac{w}{V} + \bar{C}_{n\alpha}\frac{w}{V} + \bar{C}_{m\delta}\delta_A\sin\phi + \bar{C}_{m\delta}\delta_B\cos\phi \Big] \qquad (18)$$

Results

Aerodynamic force and moment coefficients have been extracted from the free flight motion data. The analysis methodology utilized includes both linear theory and 6DOF reduction. Results are presented for 0 deg, 30 deg, 45 deg, and 60 deg offset fin conditions. Where applicable, comparisons are made to results from Reference 2 which represents the same research configuration at a typical 90 deg fin orientation.

The aerodynamic coefficients and derivatives extracted from the experimentally measured trajectories are plotted in Figures 3-6 and tabulated in Table 2. These figures show the zero angle-of-attack coefficients and derivatives obtained using the fixed plane 6DOF analysis.

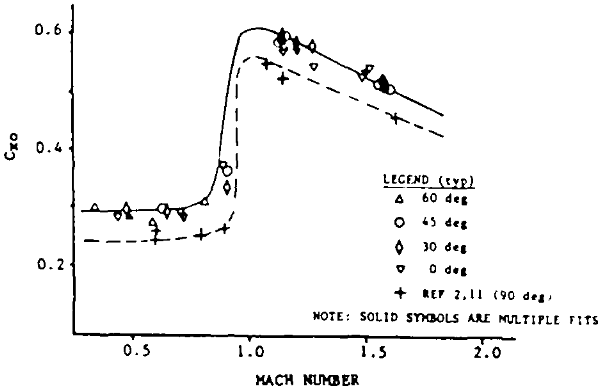

Figure 3. Zero Yaw Axial Force (C_{XO}) versus Mach number

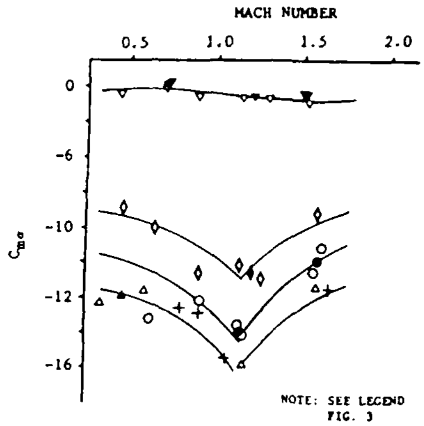

Figure 4. Pitch Moment Coefficient Derivative ($C_{m\alpha}$) versus Mach Number

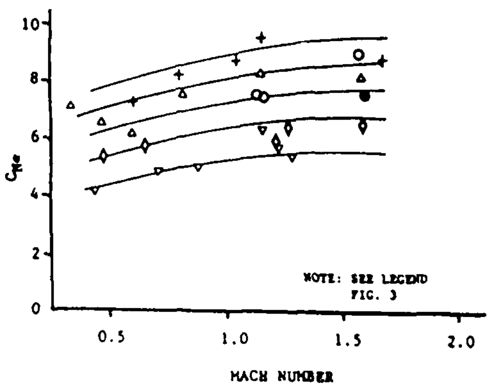

Figure 5. Normal Force Coefficient Derivative ($C_{N\alpha}$) versus Mach Number

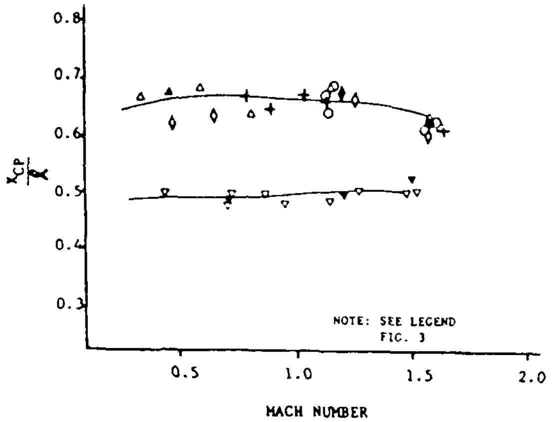

Figure 6. Center of Pressure (X_{cp}/l) versus Mach Number

The zero yaw drag plot, Figure 3, shows little difference for the four configurations tested. There was, however, a slight overall increase in drag for these offset fin models compared to the 90 deg models (ref 2,11). The discrepancy between offset fin models and 90 deg models is not understood; however, the fact that this drag remains unchanged as a function of offset fin angle indicates there is no strong drag dependence on offset fin angle.

The pitching moment coefficient derivative results for the 0-degree fin offset configuration were converted to the same C.G. location as the other fin offsets as plotted in Figure 4. The Table 2 results are presented relative to the actual model C.G. as measured. This figure indicates that there is little difference in stability between the 90 deg and 60 deg fin offset models. As fin offset angle is increased there is a steady decrease in stability to the 45 deg and 30 deg models. Then, there is a large decrease in stability from 30 deg to 0 deg. This indicates that fin effectiveness is decreasing slowly near 90 deg finn offsets followed by a sharp decrease somewhere between 30 deg and 0 deg. The normal force derivatives, Figure 5, however, show a steady decrease as a function of offset fin angle. It is also of interest to note that the data shown in Figure 6 illustrates that much of the loss in static stability for the 0 deg fin offset configuration comes from a rather dramatic forward shift of the center-of-pressure.

Figures 7-10 contain representative motion plots for each fin offset. Note the indications of dynamic instability for the 0 deg and 30 deg offsets. Based on prior research with wraparound fin configurations, the presence of out of plane moments and roll resonance conditions could be expected. The out of plane moments (side moment) could be due to; (1) the induced side moment based on the roll orientation relative to the cross-flow velocity component ($\bar{C}_{n\gamma\alpha}$ - Table 4), or (2) the moment as a function of pitch angle ($\bar{C}_{n\alpha}$ - Table 4).

In matching the observed motion, the dominant side moment was C_n . The inclusion of this aerodynamic coefficient during the data reduction process made a dramatic improvement to the quality of the fits. This was most significant for the 0 deg and 30 deg fin offsets. The trim angles were on the order of 0.5 degree and for those flights near resonance, explained the damping trends of the observed motions.

Discussion

Dynamic Stability

The resulting aerodynamic force and moment coefficients show nonlinear trends as a function of Mach number, angle of attack, and aerodynamic roll angle.

The inclusion of the side moment due to pitch angle, $C_{n\alpha}$ was critical in order to adequately fit the measured motion patterns. The tendency of the motion to develop into a circular pattern provides a clue to the possible effects of this side moment. Both Murphy[5] and Nicolaides[9] have studied the consequences of a side moment due to pitch on the dynamic stability of a finned missile. The equations for the computation of the nutational and precessional damping rates with $\bar{C}_{n\alpha}$ included are as follows:

$$\lambda_1 = \frac{\rho A}{4m}\Big[-C_{N\alpha}\left(1 - \frac{1}{\sigma}\right) + (C_{mq} + C_{m\dot{\alpha}})\left(\frac{md^2}{2I_y}\right)\left(1 + \frac{1}{\sigma}\right) + \left(\frac{md^2}{I_y}\right)\left(\frac{1}{\sigma}\right) C_{n\alpha}\left(\frac{2V}{pd}\right)\Big] \quad (19)$$

$$\lambda_2 = \frac{\rho A}{4m}\Big[-C_{N\alpha}\left(1 + \frac{1}{\sigma}\right) + (C_{mq} + C_{m\dot{\alpha}})\left(\frac{md^2}{2I_y}\right)\left(1 - \frac{1}{\sigma}\right) - \left(\frac{md^2}{I_y}\right)\left(\frac{1}{\sigma}\right) C_{n\alpha}\left(\frac{2V}{pd}\right)\Big] \quad (20)$$

where:

$$\sigma = \sqrt{1 - \frac{1}{S_g}} \quad (21)$$

$$S_g = \frac{2 I_x^2 p^2}{\pi \rho I_y C_{m\alpha} d^3 V^2} \quad (22)$$

Equations 19-20 assume that the Magnus moment is negligible. By computing the required side moment coefficient, $C_{n\alpha}$, for λ equal to zero will determine the dynamic stability boundary. This was done and the results are plotted in Figure 11 for the 0 deg and 30 deg fin offsets. The plots include Mach numbers of 0.7, 1.2, and 1.5/1.6. This shows that based on the determined side moment coefficients, a dynamic instability exists due to this moment, subsonically for these fin offsets.

Table 2. 6 DOF Aerodynamics

Single Fits

Config	Mach Number	DBSQ / ABARM	CX / CX2	CNa / CNa3	Cma / Cma3	Cmq / Cmq2	CZga3 / Cmga3	CYga3 / Cnga3	Clga2 / Cnsm	Clp / Cld	Cnda / CndB	Cmda / CmdB	Probable Error X(m) / Y-Z(m)	Probable Error Angle(deg) / Roll(deg)
60 Deg	0.335	34.4	0.298	7.02	-12.269	-416.0	0.0	0.0	0.00	-2.000	0.041	-0.015	0.0013	0.286
		9.9	0.750	0.00	0.00	0.0	0.0	0.0	0.95	0.016	0.022	0.091	0.0007	8.913
60 Deg	0.594	22.8	0.275	6.12	-11.564	-333.3	0.0	0.0	0.00	-2.000	0.000	-0.152	0.0010	0.176
		9.2	0.750	0.00	0.00	0.0	0.0	0.0	0.51	-0.005	0.000	0.016	0.0012	2.813
60 Deg	0.813	0.5	0.310	7.50	-11.030	-345.2	0.0	0.0	0.00	-2.931	0.000	0.050	0.0023	0.144
		1.3	0.750	0.00	0.00	0.0	0.0	0.0	1.13	-0.052	0.000	0.086	0.0026	9.197
60 Deg	1.160	1.8	0.579	8.25	-15.805	-292.1	0.0	0.0	0.00	-2.000	0.000	0.020	0.0019	0.162
		4.5	0.750	0.00	0.00	0.0	0.0	0.0	0.00	-0.007	0.000	0.004	0.0025	5.149
60 Deg	1.585	3.2	0.524	8.10	-11.280	-382.3	0.0	0.0	0.00	-2.000	0.000	0.018	0.0023	0.160
		5.4	0.750	0.00	0.00	0.0	0.0	0.0	0.00	-0.010	0.000	0.046	0.0024	14.740
45 Deg	0.628	5.4	0.298	7.00	-13.225	-250.0	423.0	-543.1	0.00	-4.291	0.037	-0.016	0.0020	0.389
		4.2	0.750	0.00	0.00	0.0	-981.7	462.3	-0.30	-0.010	0.034	0.085	0.0026	11.000
45 Deg	0.912	0.2	0.362	7.00	-12.139	-126.1	0.0	0.0	0.00	-2.124	0.000	-0.080	0.0030	0.194
		0.9	0.750	0.00	0.00	0.0	0.0	0.0	0.00	-0.083	0.000	-0.083	0.0021	19.630
45 Deg	1.133	0.1	0.590	7.59	-13.614	-152.5	0.0	0.0	0.00	-2.512	0.000	-0.016	0.0021	0.113
		0.8	0.750	0.00	0.00	0.0	0.0	0.0	0.00	0.030	0.000	-0.026	0.0026	7.591
45 Deg	1.153	3.8	0.598	7.30	-14.113	-264.8	0.0	0.0	0.00	-2.000	0.000	0.053	0.0028	0.205
		5.6	0.750	0.00	0.00	0.0	0.0	0.0	0.00	0.008	0.000	-0.023	0.0023	21.150
45 Deg	1.571	1.4	0.517	8.96	-10.535	-436.2	0.0	0.0	0.00	-2.000	0.000	0.074	0.0027	0.270
		3.0	0.750	0.00	0.00	0.0	0.0	0.0	0.00	0.010	0.000	-0.008	0.0023	4.965
45 Deg	1.612	0.6	0.509	6.98	-9.130	-250.0	0.0	0.0	0.00	-2.000	0.000	0.014	0.0012	0.186
		2.1	0.750	0.00	0.00	0.0	0.0	0.0	0.00	0.002	0.000	-0.017	0.0026	10.180
30 Deg	0.470	6.2	0.296	5.32	-6.897	-250.0	0.0	0.0	0.00	-2.000	0.000	-0.075	0.0006	0.323
		4.5	0.750	0.00	0.00	0.0	0.0	0.0	-1.43	-0.005	0.000	-0.082	0.0017	3.181
30 Deg	0.650	101.6	0.296	[illegible]	-8.045	-176.2	0.0	0.0	0.00	-31.349	0.000	0.118	0.0020	0.602
		18.2	0.750	[illegible]	-16.65	0.0	0.0	0.0	-0.65	-0.103	0.000	0.063	0.0022	11.360
30 Deg	0.911	1.7	0.335	7.00	-10.601	-200.6	0.0	0.0	0.00	-1.863	0.000	-0.112	0.0028	0.224
		2.2	0.750	0.00	0.00	0.0	0.0	0.0	-1.41	-0.043	0.000	-0.030	0.0020	11.880
30 Deg	1.138	0.6	0.595	8.00	-10.197	-250.0	0.0	0.0	0.00	-2.000	0.000	0.010	0.0021	0.193
		2.4	0.750	0.00	0.00	0.0	0.0	0.0	0.00	0.003	0.000	-0.005	0.0025	35.150
30 Deg	1.262	21.5	0.577	6.29	-10.975	-200.0	0.0	0.0	0.00	-10.330	0.000	0.080	0.0031	0.531
		7.9	0.750	0.00	0.00	0.0	0.0	0.0	-0.74	-0.028	0.000	0.052	0.0029	7.616
30 Deg	1.578	5.2	0.520	6.43	-7.122	-357.5	0.0	0.0	0.00	-5.426	0.000	0.038	0.0023	0.224
		5.7	0.750	0.00	0.00	0.0	0.0	0.0	-0.55	-0.045	0.000	0.024	0.0024	9.148
0 Deg	0.442	323.4	0.281	4.16	-3.933	-288.6	0.0	0.0	0.00	-9.414	0.000	-0.020	0.0019	0.392
		30.1	1.000	13.55	-47.13	0.0	0.0	0.0	-2.17	-0.101	0.000	-0.036	0.0014	15.780
0 Deg	0.705	133.8	0.292	4.84	-3.713	-100.0	0.0	0.0	0.00	0.924	0.000	0.058	0.0013	0.417
		21.4	0.833	0.00	-38.89	0.0	0.0	0.0	-1.55	-0.021	0.000	0.002	0.0014	10.660
0 Deg	0.725	341.1	0.283	3.32	-3.348	-106.8	0.0	0.0	0.00	-5.392	0.037	-0.025	0.0028	0.695
		33.5	1.000	17.07	-48.95	0.0	0.0	0.0	-1.71	-0.050	-0.039	-0.011	0.0022	16.170
0 Deg	0.884	221.5	0.375	5.06	-5.091	-100.0	0.0	0.0	0.00	3.667	0.000	-0.060	0.0020	0.644
		34.1	0.470	13.16	-76.32	0.0	0.0	0.0	-2.52	-0.018	0.000	-0.126	0.0012	9.836
0 Deg	1.147	117.8	0.573	6.29	-5.600	-253.5	0.0	0.0	0.00	-6.700	0.000	0.450	0.0026	0.497
		18.4	1.964	0.00	-51.77	0.0	0.0	0.0	-0.34	-0.064	0.000	-0.089	0.0026	14.500
0 Deg	1.280	15.0	0.542	5.38	-5.625	-244.8	0.0	0.0	0.00	0.680	0.000	-0.017	0.0028	0.305
		7.7	7.473	0.00	-35.87	0.0	0.0	0.0	-0.25	0.004	0.000	-0.013	0.0022	4.773
0 Deg	1.491	26.7	0.527	4.55	-4.500	-100.0	57.4	-33.8	0.00	-1.000	0.000	-0.029	0.0026	0.351
		9.9	3.500	0.00	-53.63	0.0	27.1	64.5	-0.47	-0.005	0.000	0.042	0.0014	5.879
0 Deg	1.523	50.8	0.546	4.70	-5.039	-109.7	33.9	137.5	0.00	-1.000	-0.021	-0.074	0.0026	0.576
		9.6	2.000	0.00	-10.04	0.0	0.0	0.0	-0.25	-0.012	-0.065	-0.161	0.0018	11.400

Multiple fits

Config	Mach Number	DBSQ / ABARM	CX / CX2 / CX4	CNa / CNa3 / CNa5	CYpa / Cnpa / Cnpa3	Cma / Cma3 / Cma5	Cmq / Cmq2 / Cmq4	CZga3 / Cmga3 / Cmga	CYga3 / Cnga3 / Cnga	Clga2 / CXga2 / Clp	CXM / CmaM / CnsM	Probable Error X(m) / Y-Z(m)	Probable Error Angle(deg) / Roll(deg)
60 Deg	0.464	29.2	0.286	6.53	0.00	-11.913	-345.3	0.0	0.0	0.00	-0.11	0.0012	0.276
		9.7	0.750	0.00	0.00	0.000	0.0	0.0	0.0	0.00	0.00	0.0010	6.269
			0.000	0.00	0.00	0.000	0.0	0.0	0.0	-2.00	0.69		
45 Deg	1.143	2.8	0.590	9.51	0.00	-13.891	-90.5	0.0	0.0	0.00	-0.07	0.0031	0.241
		5.1	0.750	0.00	0.00	0.000	0.0	0.0	0.0	0.00	0.00	0.0026	19.700
			0.000	0.00	0.00	0.000	0.0	0.0	0.0	-2.00	0.00		
45 Deg	1.592	1.0	0.513	7.51	0.00	-9.938	-577.7	0.0	0.0	0.00	-0.18	0.0020	0.223
		2.9	0.750	0.00	0.00	0.000	0.0	0.0	0.0	0.00	0.00	0.0024	7.930
			0.000	0.00	0.00	0.000	0.0	0.0	0.0	-2.00	-1.09		
30 Deg	1.200	10.7	0.589	5.90	0.00	-10.867	-200.0	0.0	0.0	0.00	-0.10	0.0028	0.419
		8.0	0.750	0.00	0.00	0.000	0.0	0.0	0.0	0.00	1.81	0.0028	29.520
			0.000	0.00	0.00	0.000	0.0	0.0	0.0	-3.34	-0.76		
0 Deg	0.715	240.4	0.295	3.67	0.00	-3.380	-17.2	0.0	0.0	0.00	0.00	0.0027	0.624
		33.4	1.000	15.39	0.00	-50.797	0.0	0.0	0.0	0.00	0.00	0.0019	13.550
			0.000	0.00	0.00	92.159	0.0	0.0	0.0	0.00	-1.48		
0 Deg	1.213	67.0	0.575	5.66	0.00	-5.535	-245.4	0.0	0.0	0.00	-0.20	0.0029	0.393
		19.0	2.194	8.30	0.00	-52.871	0.0	0.0	0.0	0.00	0.00	0.0023	10.190
			-9.705	0.00	0.00	277.160	0.0	0.0	0.0	0.00	-0.29		
0 Deg	1.507	39.1	0.533	3.40	0.00	-4.484	-109.7	46.2	13.3	0.00	-0.05	0.0028	0.470
		9.9	2.702	102.21	0.00	-41.095	0.0	6.1	57.2	0.00	0.00	0.0016	9.075
			0.000	0.00	0.00	0.000	0.0	0.0	0.0	-1.00	-0.32		

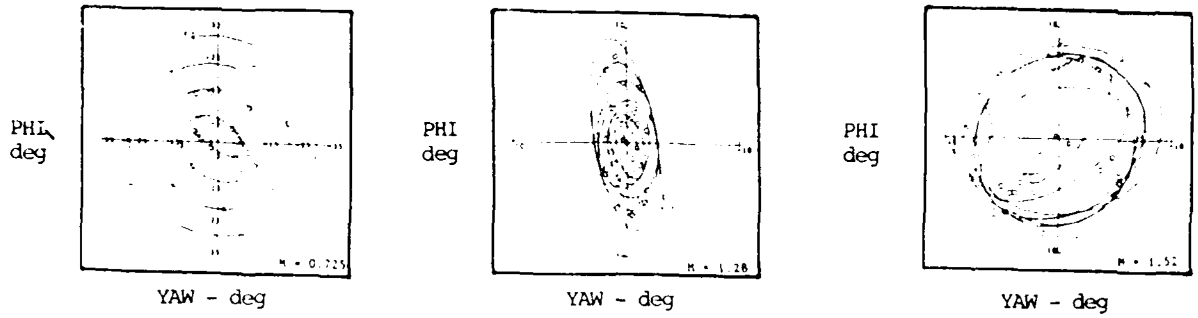

Figure 7. Motion Pattern for 0 deg Offset

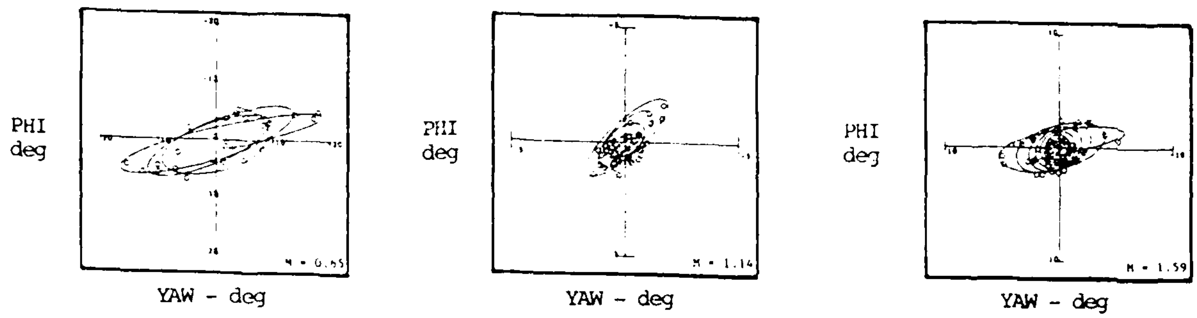

Figure 8. Motion Pattern for 30 deg Offset

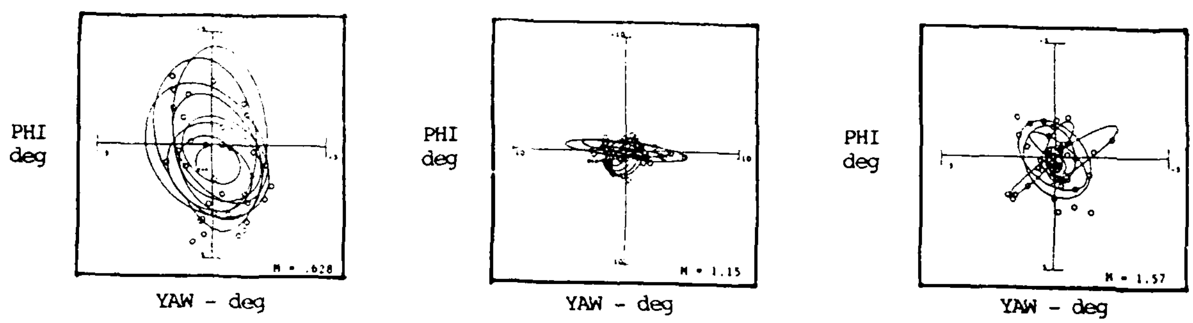

Figure 9. Motion Pattern for 45 deg Offset

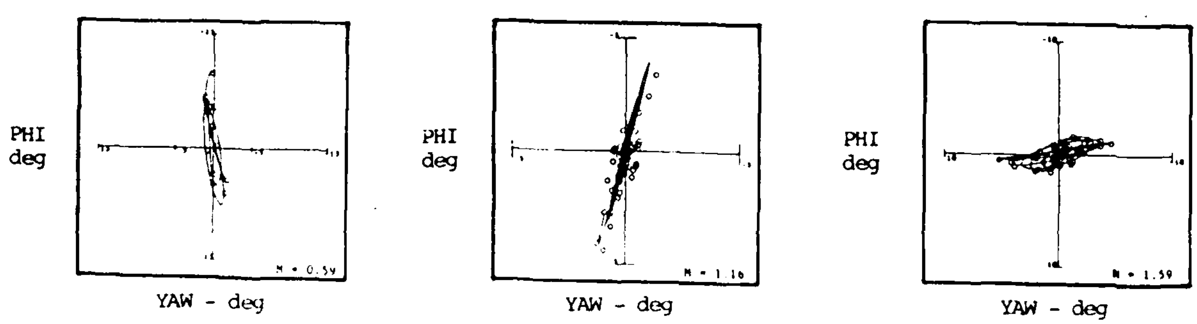

Figure 10. Motion Pattern for 60 deg Offset

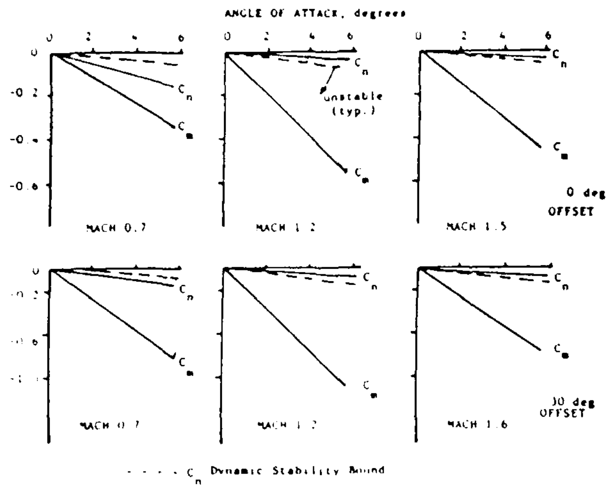

Figure 11. Stability Bounds

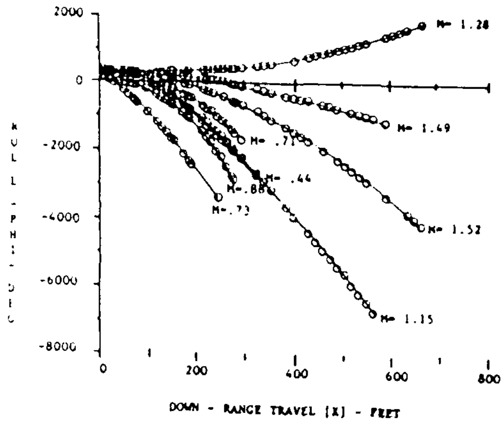

b. Present Offset Fin
(0 deg Offset)

Figure 12. (continued) Roll vs. Mach Number

Roll

There was no attempt to control spin rate for these tests. Since trim moments were determined to exist, a roll resonance condition or amplification of the trim was of concern. A combined roll resonance and side moment affect on a given flight can create such dynamic instability as to make it difficult to accurately distinguish between the two separable aerodynamic moments during the reduction process.

Previous testing on Wrap-Around Fin configurations (Ref. 7 & 10) has shown a roll dependency due to Mach number. This is shown in Figure 12 a. Here, models tested subsonically rolled in the direction of fin curvature and model tested supersonically rolled opposite the direction of fin curvature. Figure 12 b shows the roll profiles of the 0 deg offset fin configurations. These profiles indicates that there is no roll dependence due to Mach number for these offset fin configurations.

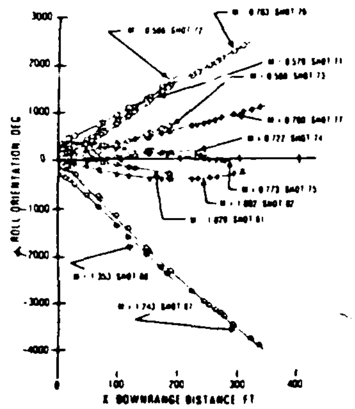

a. Wrap-Around Fin
(Ref 7, Fig. 8)

Figure 12. Roll vs. Mach Number

Conclusions

Aerodynamic and stability characteristics have been determined for four offset fin configurations.

The following summarizes the important aerodynamic characteristics:

- The change in zero yaw drag is small as the fin offset angle is varied.
- The decrease in static stability is very rapid for fin offsets below 45 deg. However, static stability is insensitive to offset fin angles of 60 deg and above.
- Dynamic instabilities due to the side moment exist subsonically for the 0 deg and 30 deg offsets. There were no indications that a destabilizing side moment existed for offset fin angles of 60 deg.
- At best, large limit cycles can be expected at fin offsets less than 45 deg due to a combination of side moment and trim moment.
- There is no roll dependence of these offset fin configurations due to Mach number.

Future research should include a more controlled spin rate environment for the tests. This will allow better isolation of the roll induced side moment, the side moment due to pitch angle, and trim moment amplification due to the spin rate approaching resonance.

References

(1) Kittyle, R.L., Packard, J.D., and Winchenbach, G.L., " Description and Capabilities Of Aeroballistic Research Facility," AFATL-TR-87-08, May 1987.

(2) West, K.O. and Whyte R.H., "Free Flight and Wind Tunnel Test of a Missile Configuration at Subsonic and Transonic Mach Numbers with

Angles of Attack up to 30 Degrees," Paper 39, 11th Navy Symposium on Aeroballistics, Tevose, PA, August 1978.

(3) Hathaway, W., "Free Flignt Data Analysis Using Maximum Likelihood Technique," Paper 545, Presented at the 28th meeting of the Aeroballistic Range Association, September 1977.

(4) Fischer, M., et. al.,"Aeroballistic Facility Data Analysis System," AFATL-TR-88-48, September 1988.

(5) Murphy, C.H., " Free Flight Motion of Symmetric Missiles," BRL Report 1216, July 1963.

(6) Murphy, C.H., " Data Reduction for the Free Flight Spark Ranges," BRL Report 900, February 1954.

(7) Winchenbach, G., Buff,R., Whyte,R., Hathaway,W. ," Subsonic and Transonic Aerodynamics of a Wraparound Fin Configuration," Journal of Guidance, Vol.9, Nov-Dec 1986,pp. 627-632.

(8) Whyte, R. and Winchenbach, G. and Hathaway, W. ," Subsonic Free Flight Data for a Complex Asymmetric Missile," Journal of Guidance , Control, and Dynamics, Vol. 4, Jan-Feb 1981,pp 59-65.

(9) Nicolaides, J., " Free Flight Dynamics," University of Notre Dame, South Bend,IN,1968.

(10) Kim, Y. and Winchenbach, G., " The Roll Motion of a Wraparound Fin Configuration at Subsonic and Transonic Mach Numbers," AIAA Paper 85-1777, Aug. 1985.

(11) Kidd, J., " An Investigation of Drag Reduction Using Stepped Afterbodies," AIAA Paper Presented at the 27th Aerospace Sciences Meeting, Janurary 1989.